PROVABLE FILTER PRUNING FOR EFFICIENT NEURAL NETWORKS

Anonymous authors
Paper under double-blind review

ABSTRACT

We present a provable, sampling-based approach for generating compact Convolutional Neural Networks (CNNs) by identifying and removing redundant filters from an over-parameterized network. Our algorithm uses a small batch of input data points to assign a saliency score for each filter and constructs an importance sampling distribution where filters that highly affect the output are sampled with correspondingly high probability. Unlike weight pruning approaches that lead to irregular sparsity patterns – requiring specialized libraries or hardware to enable computational speedups – our approach compresses the original network to a slimmer subnetwork, which enables accelerated inference with any off-the-shelf deep learning library and hardware. Existing filter pruning methods are generally data-oblivious, rely on heuristics for evaluating the parameter importance, or require manual and tedious hyper-parameter tuning. In contrast, our method is data-informed, exhibits provable guarantees on the size and performance of the pruned network, and is widely applicable to varying network architectures and data sets. Our analytical bounds bridge the notions of compressibility and importance of network structures, which gives rise to a fully-automated procedure for identifying and preserving the filters in layers that are essential to the network's performance. Our experimental results across varying pruning scenarios show that our algorithm consistently generates sparser and more efficient models than those generated by existing filter pruning approaches.

1 INTRODUCTION

Despite widespread empirical success, modern networks with millions of parameters require excessive amounts of memory and computational resources to store and conduct inference. These stringent requirements make it challenging and prohibitive to deploy large neural networks on resource-limited platforms. A popular approach to alleviate these practical concerns is to utilize a pruning algorithm to remove redundant parameters from the original, over-parameterized network. The objective of network pruning is to generate a sparse, efficient model that achieves minimal loss in predictive power relative to that of the original network.

A common practice to obtain small, efficient network architectures is to train an overparameterized network, prune it by removing the least significant weights, and re-train the pruned network (Han et al., 2015). This prune-retrain cycle is often repeated iteratively until the network cannot be pruned any further without incurring a significant loss in test accuracy relative to the original model. The computational complexity of this iterative procedure depends greatly on the effectiveness of the pruning algorithm used in identifying and preserving the essential structures of the original network.

However, modern pruning approaches[1] are generally based on heuristics (Han et al., 2015; Ullrich et al., 2017; He et al., 2018; Luo et al., 2017; Li et al., 2016; Lee et al., 2018; Yu et al., 2017a) that lack guarantees on the size and performance of the pruned network, require cumbersome ablation studies (Li et al., 2016; He et al., 2018) or manual hyper-parameter tuning (Luo et al., 2017), or heavily rely on assumptions such that parameters with large weight magnitudes are more important – which does not hold in general (Ye et al., 2018; Li et al., 2016; Yu et al., 2017a; Han et al., 2015)

In this paper, we introduce a data-informed algorithm for pruning redundant filters in Convolutional Neural Networks while incurring minimal loss in the network's accuracy (see Fig. 1 for an overview).

[1] We refer the reader to Sec. A of the appendix for additional details about the related work.

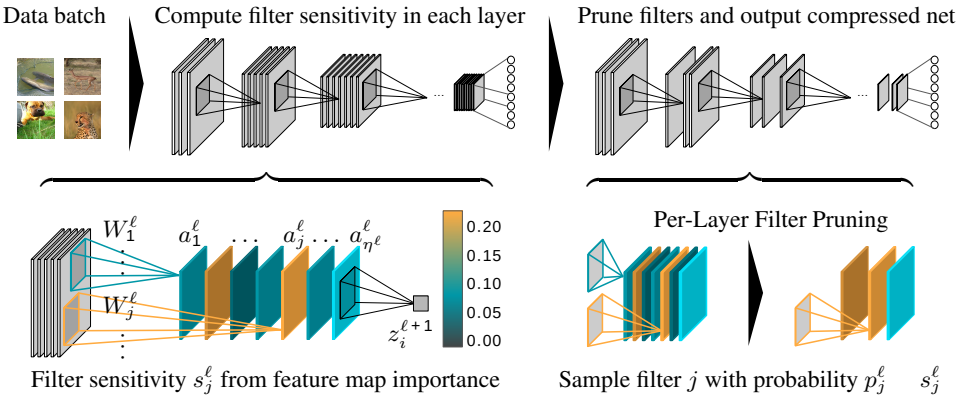

Figure 1: Overview of our pruning method. We use a small batch of data points to quantify the relative importance s_j^ℓ of each filter W_j^ℓ in layer ℓ by considering the importance of the corresponding feature map a_j^ℓ in computing the output $z^{\ell+1}$ of layer $\ell + 1$. We then prune filters by sampling each filter j with probability proportional to s_j^ℓ and removing the filters that were not sampled. We repeat the procedure for each layer and retrain once (not shown).

At the heart of our method lies a novel definition of filter importance, i.e., filter *sensitivity*, that is computed by using a small batch of input points. We prove that by empirically evaluating the relative contribution of each filter to the output of the layer, we can accurately capture its importance with respect to the other filters in the network. We show that sampling filters with probabilities proportional to their sensitivities leads to an importance sampling scheme with low variance, which enables us to establish rigorous theoretical guarantees on the size and performance of the resulting pruned network. Our analysis helps bridge the notions of compressibility and importance of each network layer: layers that are more compressible are less important for preserving the output of the original network, and vice-versa. Hence, we obtain and introduce a fully-automated sample size allocation procedure for properly identifying and preserving critical network structures as a corollary.

By pruning filters, our approach induces structured sparsity patterns, and consequently circumvents the shortcoming of existing weight-based approaches increasing test-time efficiency by generating a slimmer subnetwork that enables accelerated inference with any off-the-shelf hardware and deep learning library. We present empirical results demonstrating the effectiveness of our approach in pruning various network architectures trained on popular data sets. Our experimental results show that our approach generates sparser and more efficient models with minimal loss in accuracy when compared to those generated by state-of-the-art filter pruning approaches.

2 Sampling-based Filter Pruning

In this section, we introduce the network pruning problem and outline our sampling-based filter pruning procedure and its theoretical properties. We extend the notion of *empirical sensitivity* (Baykal et al., 2018) to quantify the importance of each filter using a small set of input points. We show that our importance criterion enables us to construct a low-variance importance sampling distribution over the filters in each layer. We conclude by showing that our approach can eliminate a large fraction of filters while ensuring that the output of each layer is approximately preserved.

2.1 Preliminaries

Consider a trained L layer network with parameters $\theta = (W^1, \ldots, W^L)$, where W^ℓ denotes the 4-dimensional tensor in layer $\ell \in [L]$, W_j^ℓ filter $j \in [\eta^\ell]$, and η^ℓ the number of filters in layer ℓ. Moreover, let $W_{:j}^{\ell+1}$ be channel j of tensor $W^{\ell+1}$ that corresponds to filter W_j^ℓ. We let $X \subseteq \mathbb{R}^d$ and $Y \subseteq \mathbb{R}^k$ denote the input and output space, respectively. The marginal distribution over the input space is given by D. For a given input $x \in X$, the output of the neural network with parameters θ is given by $f_\theta(x)$. Our overarching goal is to prune filters from each layer $\ell \in [L]$ by random sampling to generate a compact reparameterization of θ, $\hat{\theta} = (\hat{W}^1, \ldots, \hat{W}^L)$, where the number

of filters in the pruned weight tensor $\hat{W}^{\ell}$ is a small fraction of the number of filters in the original (uncompressed) tensor W^{ℓ}. Let $\mathsf{size}(\theta)$ denote the total number of parameters in the network, i.e., the sum of the number of weights over each W^{ℓ} 2 $(W^1, \ldots, W^L)$.

Pruning Objective For a given ε, δ 2 $(0, 1)$, our objective is to generate a compressed network with parameters $\hat{\theta}$ such that $\mathsf{size}(\hat{\theta})$ $\mathsf{size}(\theta)$ and $\mathsf{P}_{x \ D,\hat{\theta}}(f_{\hat{\theta}}(x)$ 2 $(1$ $\varepsilon) f_{\theta}(x))$ 1 δ, where $f_{\hat{\theta}}(x)$ 2 $(1$ $\varepsilon) f_{\theta}(x)$ denotes an entry-wise guarantee over the output neurons $f_{\hat{\theta}}(x), f_{\theta}(x)$ 2 Y R^k, i.e., the guarantee is equivalent to $f_{\hat{\theta}}(x)_i$ 2 $(1$ $\varepsilon) f_{\theta}(x)_i$ $8i$ 2 $[k]$.

2.2 Sampling Procedure

Our sampling-based filter pruning algorithm for an arbitrary layer ℓ 2 $[L]$ is depicted as Alg. 1. Note that we initially prune *channels* from $W^{\ell+1}$, but as we prune channels from $W^{\ell+1}$ we can simultaneously prune the corresponding *filters* in W^{ℓ}. The sampling procedure takes as input the set of η^{ℓ} *channels* in layer ℓ + 1 that constitute the weight tensor $W^{\ell+1}$, i.e., $W^{\ell+1}$ = $[W^{\ell+1}_{:1}, \ldots, W^{\ell+1}_{:\eta^{\ell}}]$ as well as the desired relative error and failure probability, ε, δ 2 $(0, 1)$, respectively. In Line 2 we construct the importance sampling distribution over the feature maps corresponding to the channels by leveraging the *empirical sensitivity* of each feature map j 2 $[\eta^{\ell}]$ as defined in (1) and explained in detail in the following subsections.

Algorithm 1 PruneChannels$(W^{\ell+1}, \varepsilon, \delta, s^{\ell})$

Input: $W^{\ell+1}$ = $[W^{\ell+1}_{:1}, \ldots, W^{\ell+1}_{:\eta^{\ell}}]$: original channels; ε: relative error; δ: failure probability; s^{ℓ}: feature map sensitivities as in (1)

Output: $\hat{W}^{\ell+1}$: pruned channels

1: S^{ℓ} $\sum_{j\,2\,[\eta^{\ell}]} s^{\ell}_j$ {where s^{ℓ}_j is as in (1)}
2: p^{ℓ}_j s^{ℓ}_j / S^{ℓ} $8j$ 2 $[\eta^{\ell}]$
3: m^{ℓ} $\lceil (6 + 2\varepsilon)\, S^{\ell}\, K\, \mathsf{log}(4\eta\ /\delta) \varepsilon^{\ 2} \rceil$
4: $\hat{W}^{\ell+1}$ $[0, \ldots, 0]$ {same dimensions as $W^{\ell+1}$}
5: **for** k 2 $[m^{\ell}]$ **do**
6: $c(k)$ random draw from $p^{\ell} = (p^{\ell}_1, \ldots, p^{\ell}_{\eta^{\ell}})$
7: $\hat{W}^{\ell+1}_{:c(k)}$ $\hat{W}^{\ell+1}_{:c(k)} + W^{\ell+1}_{:c(k)} / m^{\ell} p^{\ell}_{c(k)}$
8: **end for**
9: **return** $\hat{W}^{\ell+1} = [\hat{W}^{\ell+1}_{:1}, \ldots, \hat{W}^{\ell+1}_{:\eta^{\ell}}]$;

We subsequently set the sample complexity m^{ℓ} as a function of the given error (ε) and failure probability (δ) parameters in order to ensure that, after the pruning (i.e., sampling) procedure, the *approximate* output – with respect to the sampled channels $\hat{W}^{\ell+1}$ – of the layer will approximate the *true* output of the layer – with respect to the original tensor – up to a multiplicative factor of $(1$ $\varepsilon)$, with probability at least 1 δ. Intuitively, more samples are required to achieve a low specified error ε with low failure probability δ, and vice-versa. We then proceed to sample m^{l} times with replacement according to distribution p (Lines 5-8) and reweigh each sample by a factor that is inversely proportional to its sample probability to obtain an *unbiased* estimator for the layer's output (see below). We remark that m η^{ℓ} by Lemma 2, so that we only sample a small subset of the channels and discard the unsampled ones together with their corresponding filters, which leads to a reduction in the layer's size.

2.3 A Tightly-Concentrated Estimator

We now turn our attention to analyzing the influence of the sampled channels $\hat{W}^{\ell+1}$ (as constructed in Alg. 1) on layer ℓ + 1. To this end, let $z^{\ell}(x)$ and $a^{\ell}(x) = \phi(z^{\ell}(x))$ denote the pre-activation and activation of layer ℓ for an input point x to the network, respectively, where ϕ is the activation function applied entry-wise. The j^{th} feature map of layer ℓ is given by $a^{\ell}_j(x) = \phi(z^{\ell}_j(x))$. For ease of presentation, we will assume henceforth that the layer is linear[2] and will omit explicit references to the input x whenever appropriate.

Note that the *true* pre-activation of layer ℓ + 1 is given by $z^{\ell+1} = W^{\ell+1} a^{\ell}$, and the *approximate* pre-activation with respect to $\hat{W}^{\ell+1}$ is given by $\hat{z}^{\ell+1} = \hat{W}^{\ell+1} a^{\ell}$. By construction of $\hat{W}^{\ell+1}$ in Alg. 1, we equivalently have for each entry i 2 $[\eta^{\ell+1}]$ of the vector $\hat{z}^{\ell+1}$

$$\hat{z}^{\ell+1}_i = \frac{1}{m} \sum_{k=1}^{m} Y_{ik}, \quad \text{where} \quad Y_{ik} = W^{\ell+1}_{ic(k)} \frac{a^{\ell}_{c(k)}}{p^{\ell}_{c(k)}}, c(k) \quad p \quad 8k.$$

[2]The extension to CNNs follows directly as outlined Sec. B of the supplementary material.

By reweighing our samples, we obtain an unbiased estimator for each entry i of the true pre-activation output, i.e., $\mathsf{E}[\hat{z}_i^{\ell+1}] = z_i^{\ell+1}$ – which follows from linearity of expectation and the fact that $\mathsf{E}[Y_{ik}] = z_i^{\ell+1}$ for each $k \in [m]$ –, and so we have for the entire vector $\mathsf{E}_{\hat{W}^{\ell+1}}[\hat{z}^{\ell+1}] = z^{\ell+1}$. So far, we have shown that in expectation, our channel sampling procedure incurs zero error owing to its unbiasedness. However, our objective is to obtain a high probability bound on the entry-wise deviation $\left|\hat{z}_i^{\ell+1} - z_i^{\ell+1}\right|$ for each entry i, which implies that we have to show that our estimator $\hat{z}_i^{\ell+1}$ is highly concentrated around its mean $z_i^{\ell+1}$. To do so, we leverage the following standard result.

Theorem 1 (Bernstein's inequality (Vershynin, 2016)). *Let $Y_1, \ldots, Y_m$ be a sequence of m i.i.d. random variables satisfying $\max_{k\in[m]} |Y_k - \mathsf{E}[Y_k]| \leq R$, and let $Y = \sum_{k=1}^{m} Y_k$ denote their sum. Then, for every $\varepsilon > 0$, $\delta \in (0,1)$, we have that $\mathsf{P}(|Y/m - \mathsf{E}[Y_k]| \leq \varepsilon\, \mathsf{E}[Y_k]) \geq 1 - \delta$ for*

$$m \geq \frac{\log(2/\delta)}{(\varepsilon E[Y_k])^2}\left(\mathsf{Var}(Y_k) + \frac{2}{3}\varepsilon\, \mathsf{E}[Y_k] R\right).$$

Letting $i \in [\eta^{\ell+1}]$ be arbitrary and applying Theorem 1 to the mean of the random variables $(Y_{ik})_{k\in[m]}$, i.e., to $\hat{z}_i^{\ell+1}$, we observe that the number of samples required for a sufficiently high concentration around the mean is highly dependent on the magnitude and variance of the random variables $(Y_{ik})_k$. By definition of Y_{ik}, observe that these expressions are explicit functions of the sampling distribution p^ℓ. Thus, to minimize[3] the number of samples required to achieve high concentration we require a judiciously defined sampling distribution that simultaneously minimizes both R_i and $\mathsf{Var}(Y_{ik})$. For example, the naive approach of uniform sampling, i.e., $p_j^\ell = 1/\eta^\ell$ for each $j \in [\eta^\ell]$ also leads to an unbiased estimator, however, for uniform sampling we have $\mathsf{Var}(Y_{ik}) \leq \eta^\ell\, \mathsf{E}[Y_{ik}]^2$ and $R_i \leq \eta^\ell \max_k (w_{ik}^{\ell+1} a_k^\ell)$ and so $\mathsf{Var}(Y_{ik}), R \in \Omega(\eta^\ell)$ in the general case, leading to a linear sampling complexity $m \in \Omega(\eta^\ell)$ by Theorem 1.

2.4 Empirical Sensitivity (ES)

To obtain a better sampling distribution, we extend the notion of Empirical Sensitivity (ES) introduced by (Baykal et al., 2018) to prune channels. Specifically, for $W^{\ell+1} \neq 0$ (the generalization can be found in Appendix B) we let the sensitivity s_j^ℓ of feature map j in ℓ be defined as

$$s_j^\ell = \max_{x\in S} \max_{i\in[\eta^{\ell+1}]} \frac{w_{ij}^{\ell+1} a_j^\ell(x)}{\sum_{k\in[\eta^\ell]} w_{ik}^{\ell+1} a_k^\ell(x)}, \tag{1}$$

where S is a set of t independent and identically (i.i.d.) points drawn from D. Intuitively, the sensitivity of feature map $j \in [\eta^\ell]$ is the maximum (over $i \in [\eta^{\ell+1}]$) relative impact that feature map j had on any pre-activation in the next layer $z_i^{\ell+1}$. We then define the probability of sampling each channel as in Alg. 1: $j \in [\eta^\ell]$ as $p_j = s_j^\ell / S^\ell$, where $S^\ell = \sum_j s_j^\ell$ is the sum of sensitivities. Under a mild assumption on the distribution – that is satisfied by a wide class of distributions, such as the Uniform, Gaussian, Exponential, among others – of activations (Asm. 1 in Sec. B of the supplementary), ES enables us to leverage the inherent stochasticity in the draw $x \sim D$ and establish (see Lemmas 4, 5, and 6 in Sec. B) that with high probability (over the randomness in S and x) that

$$\mathsf{Var}(Y_{ik}) \in \Omega\left(S\, \mathsf{E}[Y_{ik}]^2\right) \quad \text{and} \quad R \in \Omega\left(S\, \mathsf{E}[Y_{ik}]\right) \qquad \forall i \in [\eta^{\ell+1}]$$

and that the sampling complexity is given by $m \in \Omega\left(S \log(2/\delta)\, \varepsilon^{-2}\right)$ by Theorem 1.

We note that ES does not require knowledge of the data distribution D and is easy to compute in practice by randomly drawing a small set of input points S from the validation set and passing the points in S through the network. This stands in contrast with the sensitivity framework used in state-of-the-art coresets constructions (Braverman et al., 2016; Bachem et al., 2017), where the sensitivity is defined to be with respect to the supremum over all $x \in \mathsf{supp}(D)$ in (1) instead of a maximum over $x \in S$. As also noted by Baykal et al. (2018), ES inherently considers data points that are likely to be drawn from the distribution D in practice, leading to a more practical and informed sampling distribution with lower sampling complexity.

[3] We define the minimization with respect to sample complexity from Theorem 1, which serves as a sufficiently good proxy as Bernstein's inequality is optimal up to logarithmic factors (Tropp et al., 2015).

Our insights from the discussion in this section culminate in the core theorem, which establishes that the pruned channels $\hat{W}^{\ell+1}$ (corresponding to pruned filters in W^{ℓ}) generated by Alg. 1 is such that the output of layer $\ell + 1$ is well-approximated for each entry. The proofs and additional analytical results can be found in Sec. B.

Theorem 2. *Let ε, δ 2 (0, 1), ℓ 2 [L], and let S be a set of (log (η /δ)) i.i.d. samples drawn from D. Then, $\hat{W}^{\ell+1}$ contains at most O(S^{ℓ} log(η /δ)ε ^{2})) channels and for x D, with probability at least 1 δ, we have $\hat{z}^{\ell+1}$ 2 (1 ε)$z^{\ell+1}$ (entry-wise), where η = max$_{\ell 2[L]}$ η^{ℓ}.*

Theorem 2 can be generalized and applied iteratively to obtain layer-wise approximation guarantees for the output of each layer. The resulting error can then be propagated through the layers to establish our main theorem (Thm. 8 in the supplementary) that solves the pruning problem as stated in Sec. 2.1. We refer the interested reader to the supplementary for the theorem and technical details.

3 Relative Layer Importance

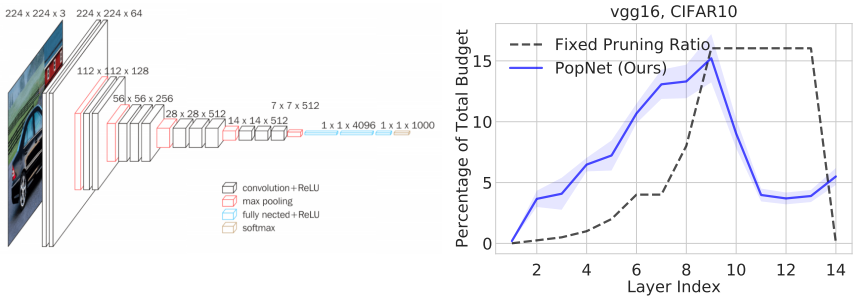

(a) VGG16 architecture

(b) Budget Allocation for VGG16

Figure 2: Early layers of VGG (Simonyan & Zisserman, 2014a) are relatively harder to approximate due to their large spatial dimensions as shown in (a). Our theoretical bounds naturally bridge compressibility and layer importance and enable us to automatically allocate relatively more samples to early layers and less to latter layers as shown in (b). The final layer's importance – due to its high influence on the final classication – is also automatically assigned a large portion of the sampling budget.

In the previous sections, we established the sampling complexity of our filter pruning scheme for any user-specified ε and δ. However, in practice, it is more common for the practitioner to specify the desired pruning ratio, which specifies the resulting size of the pruned model. Given this sampling budget, a practical question that arises is how to optimally ration the sampling budget across the network's layers to minimize the error of the pruned model. A naive approach would be to uniformly allocate the sampling budget N so that the same ratio of filters is kept in each layer. However, this allocation scheme implicitly assumes that each layer of the network is of equal importance to retaining the output, which is almost never the case in practice, as exemplified by Fig. 2(a).

It turns out that our analytical bounds on the sample complexity per layer (the expression m^{ℓ} in Alg. 1) naturally capture the importance of each layer. The key insight lies in bridging the compressibility and importance of each layer: if a layer is not very important to the output of the network, then we expect it to be highly compressible, and vice-versa. This intuition is precisely captured by our bounds that quantify the difficulty of compressibility in terms of sample complexity for that layer.

We leverage this insight to formulate a simple binary search procedure for judiciously allocating the sampling budget N as follows. Let δ be user-specified, pick a random $\varepsilon > 0$, and compute the sampling complexity m^{ℓ} as in Alg. 1 together with the resulting layer size n^{ℓ}. If $\sum_{\ell} n^{\ell} = N$, we are done, otherwise, continue searching for an appropriate ε on a smaller interval depending on whether $\sum_{\ell} n^{\ell}$ is greater or less than N. The allocation generated by this procedure, see Fig. 2(b) for an example, ensures that the maximum layer-wise error incurred by pruning is at most ε.

4 Results

We apply our pruning algorithm to a diverse set of pruning scenarios involving fully-connected and convolutional network architectures and popular data sets. We evaluate and compare our

algorithm's performance to that of state-of-the-art pruning schemes in generating a sparse and efficient models that achieve commensurate accuracy. Our evaluations show that our algorithm generates significantly smaller and efficient models when compared to those generated by competing methods. Our experimental results reaffirm the practicality and versatility of our proposed approach: across all of our experiments, our algorithm took at most 1 minute to identify and prune unimportant filters[4]. Our results show that our approach consistently generated sparser models – within commensurate accuracy of the original network – relative to those generated by competing methods on a diverse set of scenarios *without having to tune or change the hyper-parameters of our algorithm across varying scenarios*.

4.1 Experimental Setup

We compare our algorithm to that of the following filter pruning algorithms: Filter Thresholding (FT, Li et al. (2016)), SoftNet (He et al., 2018), ThiNet (Luo et al., 2017), and the approach of Huang et al. (2018), denoted by *Learn*. Our algorithm only requires two inputs in practice: the desired pruning ratio (PR) and failure probability $\delta \in (0, 1)$, since the number of samples in each layer is automatically assigned by our allocation procedure described in Sec. 3. Following the conventional data partioning ratios, we reserve 90% of the training data set for training and the remaining 10% for the validation set (Lee et al., 2018). For CIFAR10 experiments, we use the standard data augmentation techniques: padding 4 pixels on each side, random crop to 32x32 pixels, and random horizontal flip.

For each scenario, we prune the original (pre-trained) network with a target prune ratio using the respective pruning algorithm and fine-tune the network by retraining for a specified number of epochs (see Sec. E of the appendix for details). We conduct this procedure for various target prune ratios (PR) and report the percentage of parameters pruned (PR) and the percent reduction in FLOPS (FR) for each target PR. We conduct the prune-retrain cycle for a range of 20 target prune ratios, and report the highest PR and FR for which the compressed network achieves commensurate accuracy, i.e., when the pruned model's test accuracy is within 0.5% of the original model. The quantities reported are averaged over 3 trained models for each scenario, unless stated otherwise. The full details of our experimental setup and the hyper-parameters used can be found in the appendix (Sec. E).

4.2 LeNet architectures on MNIST

As our first experiment, we evaluated the performance of our pruning algorithm, denoted *PopNet*, and the comparison methods on LeNet300-100 (LeCun et al., 1998), a fully-connected network with two hidden layers of size 300 and 100 hidden units, respectively, and its convolutional counterpart, LeNet-5 (LeCun et al., 1998), which consists of two convolutional layers and two fully-connected layers. Both networks were trained on MNIST using the hyper-parameters specified in Sec. E.

[%]	Method	Err.	PR
LeNet-300-100	Unpruned	1.59	
	Ours	+0.41	**84.32**
	FT	+0.35	81.68
	SoftNet	+0.41	81.69
	ThiNet	+10.58	75.01
LeNet-5	Unpruned	0.70	
	Ours	+0.41	**88.79**
	FT	+0.46	84.05
	SoftNet	+0.40	84.03
	ThiNet	+0.31	78.89

Table 1: The prune ratio, (PR) and the corresponding test error (Err.) of our method in comparison to those of competing approaches.

Table 1 depicts the performance of each pruning algorithm in attaining the sparsest possible network that achieves commensurate accuracy for the LeNet architectures after a single prune and fine-tune step. In both scenarios, our algorithm generates significantly sparser networks compared to those generated by the competing filter pruning approaches. In fact, the pruned LeNet-5 model generated by our algorithm by removing filters achieves a prune ratio of nearly 90%, which is even competitive with the accuracy of the sparse models generated by state-of-the-art *weight pruning* algorithms (Lee et al., 2018) [5]. In addition to evaluating the sparsity of the generated models subject to the commensurate accuracy constraint, we also investigated the performance of the pruning

[4]Excluding the time required for the fine-tuning step, which was approximately the same across all methods

[5]Weight pruning approaches can generate significantly sparser models with commensurate accuracy than can filter pruning approaches since the set of feasible solutions to the problem of filter pruning is a subset of the feasible set for the weight pruning problem

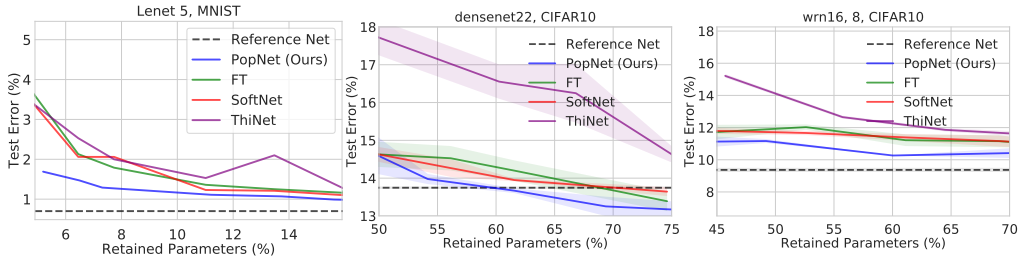

(a) LeNet5 (b) DenseNet22 (c) WRN16-8

Figure 3: The accuracy of the generated pruned models for the evaluated pruning schemes for various target prune ratios. Note that the x axis is the percentage of **parameters retained**, i.e., (1 pruneratio). Our results show that our approach generates pruned networks with minimal loss in accuracy even for low prune ratios.

	VGG16			Resnet20			Densenet22			WRN16-8		
[%]	Err.	PR	FR	Err.	PR	FR	Err.	PR	FR	Err.	PR	FR
Unpruned	8.46			8.76			13.75			9.37		
Ours	+0.48	**94.98**	**80.01**	+0.19	**47.90**	**36.60**	+0.23	**45.83**	**51.69**	+1.04	**30.00**	**31.61**
FT	-0.25*	64.0*	34.2*	+0.39	34.8	34.40	+0.45	38.5	39.52	+1.38	23.06	22.85
SoftNet	+0.84	69.88	69.87	+0.04*	10.0*	15.2*	+0.20	38.45	39.52	+1.48	23.08	22.84
ThiNet	+74.17	69.88	71.98	+1.90	37.30	37.50	+0.67	23.93	22.25	+2.71	19.75	19.72
Learn	+0.6*	83.3*	45.0*	+0.3*	27.1*	24.3*	N/A	N/A	N/A	N/A	N/A	N/A

Table 2: Overview of the pruning performance of each algorithm for various CNN architectures. For each algorithm and network architecture, the table reports the PR (%) and FR (%) of pruned models when achieving test accuracy within 0.5% of the original network's test accuracy. Our results indicate that our pruning algorithm generates smaller and more efficient networks with minimal loss in accuracy, when compared to competing approaches. (*) denotes the results reported in the original paper.

algorithms for extreme (i.e., $< 5\%$) pruning ratios (see Fig. 3). Fig. 3 we see that our algorithm's performance relative to those of competing algorithms is strictly better for a wide range of target prune ratios. For LeNet-5, for example, Fig. 3 shows that our algorithm's favorable performance is even more pronounced at extreme sparsity levels (at 95% prune ratio).

4.3 Convolutional Neural Networks on CIFAR-10

Next, we evaluated the performance of each pruning algorithm on significantly larger and deeper Convolutional Neural Networks trained on the CIFAR-10 data set: VGG16 (Simonyan & Zisserman, 2014a), ResNet20 (He et al., 2016), DenseNet22 (Huang et al., 2017), and WideResNet16-8 (Zagoruyko & Komodakis, 2016). Our results are summarized in Table 2 and Figure 3. We note that PR and FR values with an asterix (*) in Table 2 were taken directly from the results reported in the respective paper that introduced the corresponding algorithm. Similar to the results reported in Table 1 in the previous subsection, Table 2 shows that our method is able to achieve the most sparse model with minimal loss in predictive power relative to the original network. Furthermore, by inspecting the values reported for Flops Retained (FR), we observe that the models generated by our approach are not only more sparse in terms of the number of total parameters, but also more efficient in terms of the inference time complexity.

Fig. 3 depicts the performance of the evaluated algorithms for various levels of prune ratios. Once again, we see the consistently better performance of our algorithm in generating sparser models that approximately match the predictive power of the original uncompressed network. In view of our results from the previous subsection, the results in shown in Table 2 and Fig. 3 highlight the versatility and broad applicability of our method, and seem to suggest that our approach fares better relative to the compared algorithms on more challenging pruning tasks. We suspect that this could be explained by the data-informed evaluations of filter importance – which makes our algorithm robust to variations in architecture and data distributions – and the theoretical guarantees that our method exhibits, which ensure favorable and consistent performance for any pruning scenarios.

4.4 APPLICATION TO REAL-TIME REGRESSION TASKS

Real-time applications of neural networks, such as their use in autonomous driving scenarios, require network models that are not only highly accurate, but also highly efficient, i.e., fast, when it comes to inference time complexity (Amini et al., 2018). Model compression, and in particular, filter pruning has potential to generate compressed networks capable of achieving both of these objectives. To evaluate and compare the effectiveness of our method on pruning networks intended for regression tasks and real-time systems, we evaluated the various pruning approaches on the *DeepKnight* network (Amini et al., 2018), a regression network deployed on an autonomous vehicle in real time to predict the steering angle of the human driver (see E.4 in appendix for experimental details).

Fig. 4 depicts the results of our evaluations and comparisons on the *DeepKnight* network *without* the fine-tuning step. We omitted the fine-tuning step for this scenario because (i) the evaluated algorithms were able to generate highly accurate models without the retraining step and (ii) in order to evaluate and compare the performance of solely the core pruning procedure. Similar to the results obtained in the preceding pruning scenarios, Fig. 4 shows that our method consistently outperforms competing approaches for all of the specified prune ratios.

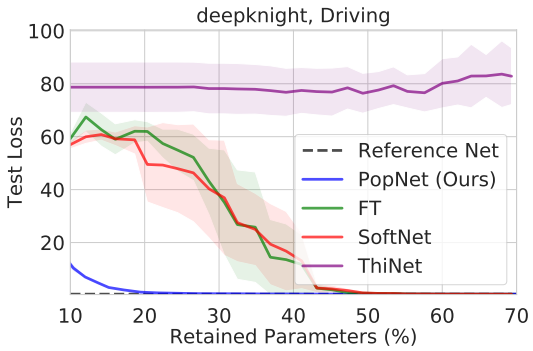

Figure 4: The performance of our approach (PopNet) and competing approaches on network for the real-time regression task used to infer the steering angle for an autonomous driving task.

4.5 DISCUSSION

In addition to the favorable empirical results of our algorithm, our approach exhibits various advantages over competing methods that manifest themselves in our empirical evaluations. For one, our algorithm does not require any additional hyper-parameters other than the pruning ratio and the desired failure probability. Given these sole two parameters, our approach automatically allocates the number of filters to sample for each layer. This alleviates the need to perform time-intensive ablation studies (He et al., 2018) and to resort to uninformed (i.e., uniform) sample allocation strategies, e.g., removing the same percentage of filters in each layer (Li et al., 2016), which fails to consider the non-uniform influence of each layer on the network's output (see Sec. 3). Moreover, our algorithm is simple-to-implement and computationally efficient both in theory and practice: the computational complexity is dominated by the jSj forward passes required to compute the sensitivities (jSj 256 in practical settings) and in practice, our algorithm takes on the order of a minute to prune the network.

5 CONCLUSION

We presented – to the best of our knowledge – the first filter pruning algorithm that generates a pruned network with theoretical guarantees on the size and performance of the generated network. Our method is data-informed, simple-to-implement, and efficient both in theory and practice. Our approach can also be broadly applied to varying network architectures and data sets with minimal hyper-parameter tuning necessary. This stands in contrast to existing filter pruning approaches that are generally based on heuristics and may require tedious hyper-parameter tuning. Our experimental results reaffirm the favorable properties of our approach in obtaining sparse, efficient networks with commensurate predictive power relative to the original uncompressed network. We conjecture that our algorithm and analysis can be leveraged to gain further insights into the properties of modern networks, such as their generalization properties.

REFERENCES

Dimitris Achlioptas, Zohar Karnin, and Edo Liberty. Matrix entry-wise sampling: Simple is best. *Submitted to KDD*, 2013(1.1):1–4, 2013. 16

Jose M Alvarez and Mathieu Salzmann. Compression-aware training of deep networks. In *Advances in Neural Information Processing Systems*, pp. 856–867, 2017. 12

Alexander Amini, Liam Paull, Thomas Balch, Sertac Karaman, and Daniela Rus. Learning steering bounds for parallel autonomous systems. In *2018 IEEE International Conference on Robotics and Automation (ICRA)*, pp. 1–8. IEEE, 2018. 8, 23, 24

Sanjeev Arora, Rong Ge, Behnam Neyshabur, and Yi Zhang. Stronger generalization bounds for deep nets via a compression approach. *arXiv preprint arXiv:1802.05296*, 2018. 12

Olivier Bachem, Mario Lucic, and Andreas Krause. Practical coreset constructions for machine learning. *arXiv preprint arXiv:1703.06476*, 2017. 4, 16

Cenk Baykal, Lucas Liebenwein, Igor Gilitschenski, Dan Feldman, and Daniela Rus. Data-dependent coresets for compressing neural networks with applications to generalization bounds. *arXiv preprint arXiv:1804.05345*, 2018. 2, 4, 12, 13, 14, 16, 21

Cenk Baykal, Lucas Liebenwein, Igor Gilitschenski, Dan Feldman, and Daniela Rus. Sipping neural networks: Sensitivity-informed provable pruning of neural networks. *arXiv preprint*, 2019. 12

Vladimir Braverman, Dan Feldman, and Harry Lang. New frameworks for offline and streaming coreset constructions. *arXiv preprint arXiv:1612.00889*, 2016. 4, 16

Wenlin Chen, James T. Wilson, Stephen Tyree, Kilian Q. Weinberger, and Yixin Chen. Compressing neural networks with the hashing trick. *CoRR*, abs/1504.04788, 2015. URL http://arxiv.org/abs/1504.04788. 12

Anna Choromanska, Krzysztof Choromanski, Mariusz Bojarski, Tony Jebara, Sanjiv Kumar, and Yann LeCun. Binary embeddings with structured hashed projections. In *International Conference on Machine Learning*, pp. 344–353, 2016. 12

Emily Denton, Wojciech Zaremba, Joan Bruna, Yann LeCun, and Rob Fergus. Exploiting linear structure within convolutional networks for efficient evaluation. *CoRR*, abs/1404.0736, 2014. URL http://arxiv.org/abs/1404.0736. 12

Petros Drineas and Anastasios Zouzias. A note on element-wise matrix sparsification via a matrix-valued bernstein inequality. *Information Processing Letters*, 111(8):385–389, 2011. 16

Dan Feldman and Michael Langberg. A unified framework for approximating and clustering data. In *Proceedings of the forty-third annual ACM symposium on Theory of computing*, pp. 569–578. ACM, 2011. 16

Yiwen Guo, Anbang Yao, and Yurong Chen. Dynamic network surgery for efficient dnns. In *Advances In Neural Information Processing Systems*, pp. 1379–1387, 2016. 12

Song Han, Huizi Mao, and William J. Dally. Deep compression: Compressing deep neural network with pruning, trained quantization and huffman coding. *CoRR*, abs/1510.00149, 2015. URL http://arxiv.org/abs/1510.00149. 1, 12

Kaiming He, Xiangyu Zhang, Shaoqing Ren, and Jian Sun. Deep residual learning for image recognition. In *Proceedings of the IEEE conference on computer vision and pattern recognition*, pp. 770–778, 2016. 7, 22

Yang He, Guoliang Kang, Xuanyi Dong, Yanwei Fu, and Yi Yang. Soft filter pruning for accelerating deep convolutional neural networks. *arXiv preprint arXiv:1808.06866*, 2018. 1, 6, 8, 12, 22

Gao Huang, Zhuang Liu, Laurens Van Der Maaten, and Kilian Q Weinberger. Densely connected convolutional networks. In *Proceedings of the IEEE conference on computer vision and pattern recognition*, pp. 4700–4708, 2017. 7, 22

Qiangui Huang, Kevin Zhou, Suya You, and Ulrich Neumann. Learning to prune filters in convolutional neural networks. *arXiv preprint arXiv:1801.07365*, 2018. 6, 22

Yani Ioannou, Duncan Robertson, Jamie Shotton, Roberto Cipolla, and Antonio Criminisi. Training cnns with low-rank filters for efficient image classification. *arXiv preprint arXiv:1511.06744*, 2015. 12

Max Jaderberg, Andrea Vedaldi, and Andrew Zisserman. Speeding up convolutional neural networks with low rank expansions. *arXiv preprint arXiv:1405.3866*, 2014. 12

Abhisek Kundu and Petros Drineas. A note on randomized element-wise matrix sparsification. *arXiv preprint arXiv:1404.0320*, 2014. 16

Yann LeCun, John S Denker, and Sara A Solla. Optimal brain damage. In *Advances in neural information processing systems*, pp. 598–605, 1990. 12

Yann LeCun, Léon Bottou, Yoshua Bengio, and Patrick Haffner. Gradient-based learning applied to document recognition. *Proceedings of the IEEE*, 86(11):2278–2324, 1998. 6, 22

Namhoon Lee, Thalaiyasingam Ajanthan, and Philip HS Torr. Snip: Single-shot network pruning based on connection sensitivity. *arXiv preprint arXiv:1810.02340*, 2018. 1, 6, 12

Hao Li, Asim Kadav, Igor Durdanovic, Hanan Samet, and Hans Peter Graf. Pruning filters for efficient convnets. *arXiv preprint arXiv:1608.08710*, 2016. 1, 6, 8, 12, 22

Jian-Hao Luo, Jianxin Wu, and Weiyao Lin. Thinet: A filter level pruning method for deep neural network compression. In *Proceedings of the IEEE international conference on computer vision*, pp. 5058–5066, 2017. 1, 6, 22

Shannon McCurdy. Ridge regression and provable deterministic ridge leverage score sampling. In *Advances in Neural Information Processing Systems*, pp. 2463–2472, 2018. 16

Dimitris Papailiopoulos, Anastasios Kyrillidis, and Christos Boutsidis. Provable deterministic leverage score sampling. In *Proceedings of the 20th ACM SIGKDD international conference on Knowledge discovery and data mining*, pp. 997–1006. ACM, 2014. 16

Adam Paszke, Sam Gross, Soumith Chintala, Gregory Chanan, Edward Yang, Zachary DeVito, Zeming Lin, Alban Desmaison, Luca Antiga, and Adam Lerer. Automatic differentiation in pytorch. In *NIPS-W*, 2017. 21

Qinfeng Shi, James Petterson, Gideon Dror, John Langford, Alex Smola, and SVN Vishwanathan. Hash kernels for structured data. *Journal of Machine Learning Research*, 10(Nov):2615–2637, 2009. 12

Karen Simonyan and Andrew Zisserman. Very deep convolutional networks for large-scale image recognition. *CoRR*, abs/1409.1556, 2014a. URL http://arxiv.org/abs/1409.1556. 5, 7

Karen Simonyan and Andrew Zisserman. Very deep convolutional networks for large-scale image recognition. *arXiv preprint arXiv:1409.1556*, 2014b. 22

Joel A Tropp et al. An introduction to matrix concentration inequalities. *Foundations and Trends® in Machine Learning*, 8(1-2):1–230, 2015. 4, 16

Karen Ullrich, Edward Meeds, and Max Welling. Soft weight-sharing for neural network compression. *arXiv preprint arXiv:1702.04008*, 2017. 1, 12

Ramon van Handel. Probability in high dimension. Technical report, PRINCETON UNIV NJ, 2014. 19

Roman Vershynin. High-dimensional probability. *An Introduction with Applications*, 2016. 4, 21

Kilian Q. Weinberger, Anirban Dasgupta, Josh Attenberg, John Langford, and Alexander J. Smola. Feature hashing for large scale multitask learning. *CoRR*, abs/0902.2206, 2009. URL http://arxiv.org/abs/0902.2206. 12

Jianbo Ye, Xin Lu, Zhe Lin, and James Z Wang. Rethinking the smaller-norm-less-informative assumption in channel pruning of convolution layers. *arXiv preprint arXiv:1802.00124*, 2018. 1, 12

Ruichi Yu, Ang Li, Chun-Fu Chen, Jui-Hsin Lai, Vlad I Morariu, Xintong Han, Mingfei Gao, Ching-Yung Lin, and Larry S Davis. Nisp: Pruning networks using neuron importance score propagation. *Preprint at https://arxiv. org/abs/1711.05908*, 2017a. 1, 12

Xiyu Yu, Tongliang Liu, Xinchao Wang, and Dacheng Tao. On compressing deep models by low rank and sparse decomposition. In *Proceedings of the IEEE Conference on Computer Vision and Pattern Recognition*, pp. 7370–7379, 2017b. 12

Sergey Zagoruyko and Nikos Komodakis. Wide residual networks. *arXiv preprint arXiv:1605.07146*, 2016. 7, 22

Liang Zhao, Siyu Liao, Yanzhi Wang, Jian Tang, and Bo Yuan. Theoretical properties for neural networks with weight matrices of low displacement rank. *CoRR*, abs/1703.00144, 2017. URL http://arxiv.org/abs/1703.00144. 12

A Related Work

General network compression The need to tame the excessive storage requirements and costly inference associated with large, over-parameterized networks has led to a rich body of work in network pruning and compression. These approaches range from those inspired by classical tensor decompositions (Yu et al., 2017b; Jaderberg et al., 2014; Denton et al., 2014), and random projections and hashing (Arora et al., 2018; Ullrich et al., 2017; Chen et al., 2015; Weinberger et al., 2009; Shi et al., 2009) that compress a pre-trained network, to those approaches that enable sparsity by embedding sparsity as an objective directly in the training process (Ioannou et al., 2015; Alvarez & Salzmann, 2017) or exploit tensor structure to induce sparsity (Choromanska et al., 2016; Zhao et al., 2017). Overall, the predominant drawback of these methods is that they require laborious hyperparameter tuning, lack rigorous theoretical guarantees on the size and performance of the resulting compressed network, and/or conduct compression in a data oblivious way.

Weight-based pruning A large subset of modern pruning algorithms fall under the general approach of pruning individual weights of the network by assigning each weight a saliency score, e.g., its magnitude (Han et al., 2015), and subsequently inducing sparsity by deterministically removing those weights below a certain saliency score threshold (Guo et al., 2016; Han et al., 2015; Lee et al., 2018; LeCun et al., 1990). These approaches are heuristics that do not provide any theoretical performance guarantees and generally require – with the exception of (Lee et al., 2018) – computationally expensive train-prune-retrain cycles and tedious hyper-parameter tuning. Unlike our approach that enables accelerated inference (i.e., reduction in FLOPS) on any hardware and with any deep learning library by generating a smaller subnetwork, weight-based pruning generates a model with non-structured sparsity that requires specialized hardware and sparse linear algebra libraries in order to speed up inference.

Neuron pruning Pruning entire neurons in FNNs and filters in CNNs is particularly appealing as it shrinks the network into its slimmer counterpart, which leads to alleviated storage requirements and improved inference-time performance on any hardware. Similar to the weight-based approaches, approaches in this domain assign an importance score to each neuron or filter and remove those with a score below a certain threshold (He et al., 2018; Li et al., 2016; Yu et al., 2017a). These approaches generally take the ℓ_p norm –with $p = \{1, 2\}$ as popular choices– of the filters to assign filter importance and subsequently prune unimportant filers. These methods are data-oblivious heuristics that heavily rely on the assumption that filters with large weight magnitudes are more important, which may not hold in general (Ye et al., 2018).

In general, prior work on neuron and filter pruning has focused on approaches that lack theoretical guarantees and a principled approach to allocating the sampling budget across layers, requiring tedious ablation studies or settling for naive uniform allocation across the layers. In contrast to prior approaches, our algorithm assigns data-informed saliency scores to filters, guarantees an error bound, and leverages our theoretical error bounds to automatically identify important layers and allocate the user-specified sampling budget (i.e., pruning ratio) across the layers.

Our work is most similar to that of (Baykal et al., 2018; 2019), which proposed an weight pruning algorithm with provable guarantees that samples weights of the network in accordance to an empirical notion of parameter importance. The main drawback of their approach is the limited applicability to only fully-connected networks, and the lack of inference-time acceleration due to non-structured sparsity caused by removing individual weights. Our method is also sampling-based and relies on a data-informed notion of importance, however, unlike (Baykal et al., 2018; 2019), our approach can be applied to both FNNs and CNNs and generates sparse, efficient subnetworks that accelerate inference.

B Algorithmic and Analytical Details

Algorithm 2 is the full algorithm for pruning features, i.e., neurons in fully-connected layers and channels in convolutional layers. For notational simplicity, we will derive our theoretical results for linear layers, i.e., neuron pruning. We remind the reader that this result also applies to CNNs by taking channels of a weight tensor in place of neurons. The pseudocode is organized for clarity of exposition rather than computational efficiency. Recall that θ is the full parameter set of the net,

where $W^\ell \in \mathbb{R}^{\eta^\ell \times \eta^{\ell+1}}$ is the weight matrix between layers ℓ and $\ell+1$. W^ℓ_k refers to the k^{th} neuron of W^ℓ.

Algorithm 2 PRUNECHANNELS$(\theta, \ell, S, \varepsilon, \delta)$ - *extended version*

Input: θ: trained net; $\ell \in [L]$: layer; $S \subseteq \text{supp}(D)$: sample of inputs; $\varepsilon \in (0,1)$: accuracy; $\delta \in (0,1)$: failure probability

Output: $\hat{W}^\ell$: filter-reduced weight tensor for layer ℓ; $\hat{W}^{\ell+1}$: channel reduced, weight tensor for layer $\ell+1$

1: **for** $j \in [\eta^\ell]$ **do**
2: **for** $i \in [\eta^{\ell+1}]$ and $\mathbf{x} \in S$ **do**
3: $I^+ \leftarrow \{j \in [\eta^\ell] : w^{\ell+1}_{ij} a^\ell_j(\mathbf{x}) > 0\}$
4: $I \leftarrow [\eta^\ell] \cap I^+$
5: $g^{\ell+1}_{ij}(\mathbf{x}) \leftarrow \max_{I \subseteq \{I^+, I\}} \frac{w^{\ell+1}_{ij} a^\ell_j(\mathbf{x})}{\sum_{k \in I} w^{\ell+1}_{ik} a^\ell_k(\mathbf{x})}$
6: **end for**
7: $s^\ell_j \leftarrow \max_{\mathbf{x} \in S} \max_{i \in [\eta^{\ell+1}]} g^{\ell+1}_{ij}(\mathbf{x})$
8: **end for**
9: $S^\ell \leftarrow \sum_{j \in [\eta^\ell]} s^\ell_j$
10: **for** $j \in [\eta^\ell]$ **do**
11: $p^\ell_j \leftarrow s^\ell_j / S^\ell$
12: **end for**
13: $K \leftarrow$ value from Assumption 1
14: $m \leftarrow \lceil (6+2\varepsilon) S^\ell K \log(2\eta^{\ell+1}/\delta) \varepsilon^{-2} \rceil$
15: $H \leftarrow$ distribution on $[\eta^\ell]$ assigning probability p^ℓ_j to index j
16: $\hat{W}^\ell \leftarrow (0, \ldots, 0)$ {same dimensions as W^ℓ}
17: $\hat{W}^{\ell+1} \leftarrow (0, \ldots, 0)$ {same dimensions as $W^{\ell+1}$}
18: **for** $k \in [m]$ **do**
19: $c(k) \leftarrow$ random draw from H
20: $\hat{W}^\ell_{c(k)} \leftarrow W^\ell_{c(k)}$ {no reweighing or considering multiplicity of drawing index $c(k)$ multiple times}
21: $\hat{W}^{\ell+1}_{:c(k)} \leftarrow \hat{W}^{\ell+1}_{:c(k)} + \frac{W^{\ell+1}_{:c(k)}}{m p_{c(k)}}$ {reweighing for unbiasedness of pre-activation in layer $\ell+1$}
22: **end for**
23: **return** $\hat{W}^\ell = [\hat{W}^\ell_1, \ldots, \hat{W}^\ell_{\eta^\ell}]$; $\hat{W}^{\ell+1} = [\hat{W}^{\ell+1}_{:1}, \ldots, \hat{W}^{\ell+1}_{:\eta^\ell}]$

Recall that $z^{\ell+1}_i(\mathbf{x})$ denotes the pre-activation of the i^{th} neuron in layer $\ell+1$ given input $\mathbf{x}$, and the activation $a^\ell_j(x) = \max\{0, z^\ell_j(\mathbf{x})\}$.

Definition 1 (Edge Sensitivity (Baykal et al., 2018))**.** *Fixing a layer $\ell \in [L]$, let $w^{\ell+1}_{ij}$ be the weight of edge $(j,i) \in [\eta^\ell] \times [\eta^{\ell+1}]$. The empirical sensitivity of weight entry $w^{\ell+1}_{ij}$ with respect to input $\mathbf{x} \in X$ is defined to be*

$$g^{\ell+1}_{ij}(\mathbf{x}) = \max_{I \subseteq \{I^+, I\}} \frac{w^{\ell+1}_{ij} a^\ell_j(\mathbf{x})}{\sum_{k \in I} w^{\ell+1}_{ik} a^\ell_k(\mathbf{x})}, \tag{2}$$

where $I^+ = \{j \in [\eta^\ell] : w^{\ell+1}_{ij} a^\ell_j(\mathbf{x}) > 0\}$ and $I = [\eta^\ell] \cap I^+$ denote the set of positive and negative edges, respectively.

Algorithm 2 uses empirical sensitivity to compute the sensitivity of neurons on Lines 9-12.

Definition 2 (Neuron Sensitivity)**.** *The sensitivity of a neuron $j \in [\eta^\ell]$ in layer ℓ is defined as*

$$s^\ell_j = \max_{\mathbf{x} \in S} \max_{i \in [\eta^{\ell+1}]} g^{\ell+1}_{ij}(\mathbf{x}) \tag{3}$$

In this section, we prove that Algorithm 2 yields a good approximation of the original net. We begin with a mild assumption to ensure that the distribution of our input is not pathological.

Assumption 1. *There exist universal constants $K, K' > 0$ such that for any layer ℓ and all $j \in [\eta^\ell]$, the CDF of the random variable $\max_{i \in [\eta^{\ell+1}]} g^{\ell+1}_{ij}(x)$ for $x \sim D$, denoted by $F_j(\cdot)$, satisfies*

$$F_j(M_j/K) \geq 1 - \exp(-1/K'),$$

where $M_j = \min\{y \in [0,1] : F_j(y) = 1\}$.

Note that the analysis is carried out for the positive and negative elements of $W^{\ell+1}$ separately, which is also considered in the definition of sensitivity (Def. 1). For ease of exposition, we will thus assume that throughout the section $W^{\ell+1}$ 0 (element-wise), i.e., $I^+ = [\eta^\ell]$, and derive the results for this case. However, we note that we could equivalently assume $W^{\ell+1}$ 0 and the analysis would hold regardless. By considering both the positive and negative parts of $W^{\ell+1}$ in Def. 1 we can carry out the analysis for weight tensors with positive and negative elements.

Theorem 2. *Let ε, δ 2 (0, 1), ℓ 2 [L], and let S be a set of* (log (η /δ)) *i.i.d. samples drawn from D. Then, $\hat{W}^{\ell+1}$ contains at most $O(S^\ell \log(\eta/\delta)\varepsilon^{-2})$ channels and for x D, with probability at least 1 δ, we have $\hat{z}^{\ell+1}$ 2 (1 ε)$z^{\ell+1}$ (entry-wise), where η = $\max_{\ell 2[L]} \eta^\ell$.*

The remainder of this section builds towards proving Theorem 2. We begin by fixing a layer ℓ 2 [L] and neuron i 2 [$\eta^{\ell+1}$]. Consider the random variables $fY_k g_{k2[m]}$ where $Y_k(\mathbf{x}) = \frac{1}{mp_j} w_{ij}^{\ell+1} a_j^\ell(\mathbf{x})$ where Algorithm 2 selected index j 2 [η^ℓ] on the k^{th} iteration of Line 19. Note that $z_i^{\ell+1}(\mathbf{x}) = \sum_{j2[\eta^\ell]} w_{ij}^{\ell+1} a_j^\ell(\mathbf{x})$ and so we may also write $g_{ij}^{\ell+1}(\mathbf{x}) = w_{ij}^{\ell+1} a_j^\ell(\mathbf{x}) / z_i^{\ell+1}(\mathbf{x})$ when it is more convenient.

Lemma 3. *For each $\mathbf{x}$ 2 X and k 2 [m], $\mathsf{E}[Y_k(\mathbf{x})] = z_i^{\ell+1}(\mathbf{x})/m$.*

Proof. Y_j is drawn from distribution H defined on Line 15, so we compute the expectation directly.

$$\begin{aligned}
\mathsf{E}[Y_j(\mathbf{x})] &= \sum_{k2[\eta^\ell]} \frac{w_{ik}^{\ell+1} a_k^\ell(\mathbf{x})}{m\, p_k} \quad p_k \\
&= \frac{1}{m} \sum_{k2[\eta^\ell]} w_{ik}^{\ell+1} a_k^\ell(\mathbf{x}) \\
&= \frac{z_i^{\ell+1}(\mathbf{x})}{m}
\end{aligned}$$

□

To bound the variance, we use an approach inspired by Baykal et al. (2018) where the main idea is to use the notion of empirical sensitivity to establish that a particular useful inequality holds with high probability over the randomness of the input point x D. Given that the inequality holds we can establish favorable bounds on the variance and magnitude of the random variables, which lead to a low sampling complexity.

For a random input point $\mathbf{x}$ D, let G denote the event that the following inequality holds (for all neurons):

$$\max_{i2[\eta^{\ell+1}]} g_{ij}^{\ell+1}(\mathbf{x}) \quad C\, s_j \quad 8j \text{ 2 } [\eta^\ell]$$

where C = max$f3K, 1g$ and K is defined as in Assumption 1. We now prove that under Assumption 1, event G occurs with high probability. From now on, to ease notation, we will drop certain superscripts/subscripts with the meaning is clear. For example, $z(\mathbf{x})$ will refer to $z_i^{\ell+1}(\mathbf{x})$.

Lemma 4. *If Assumption 1 holds, $\mathsf{P}(G) > 1$ $\delta/2\eta^\ell$. Here the probability is over the randomness of drawing $\mathbf{x}$ D.*

Proof. Since $\max_{i2[\eta^{\ell+1}]} g_{ij}(x)$ is just a function of the random variable x D, for any j 2 [η^ℓ] we can let D be a distribution over $\max_{i2[\eta^{\ell+1}]} g_{ij}(x)$ and observe that since $s_j = \max_{\mathbf{x}2S} \max_{i2[\eta^{\ell+1}]} g_{ij}(\mathbf{x})$, the negation of event G for a single neuron j 2 [η^ℓ] can be expressed as the event

$$X > C \max_{k2[jSj]} X_k,$$

where X D and $X_1, \ldots, X_{jSj} \overset{i.i.d.}{} D$ since the points in S were drawn i.i.d. from D. Invoking Lemma 8 from Baykal et al. (2018) in conjunction with Assumption 1, we obtain for any arbitrary j

$$\mathsf{P}(\max_{i2[\eta^{\ell+1}]} g_{ij}(x) > C\, s_j) = \mathsf{P}(X > C \max_{k2[jSj]} X_k) \quad \exp(\ jSj/K^0)$$

with the K^0 from Assumption 1. Since our choice of neuron j was arbitrary, the inequality above holds for all neurons, therefore we can apply the union bound to obtain:

$$\begin{aligned}
\mathop{\mathsf{P}}_{x\ D}(\mathsf{G}) = 1 \quad & \mathsf{P}(9j\ 2\ [\eta^\ell] : \max_{i2[\eta^{\ell+1}]} g_{ij}(x) > C\, s_j) \\
1 \quad & \sum_{j2[\eta^\ell]} \mathsf{P}(\max_{i2[\eta^{\ell+1}]} g_{ij}(x) > C\, s_j) \\
1 \quad & \eta^\ell \exp(\quad jSj/K^0) \\
1 \quad & \frac{\delta}{2\eta^{\ell+1}}
\end{aligned}$$

where the last line follows from the fact that $jSj \quad \lceil K^0 \log\left(2\,\eta^\ell \eta^{\ell+1}/\delta\right) \rceil$. □

Lemma 5. *For any* $\mathbf{x}$ *such that event* G *occurs, then* $jY_k(\mathbf{x}) \quad \mathsf{E}[Y_k(\mathbf{x})]j \quad CSz/m$. *Here the expectation is over the randomness of Algorithm 2.*

Proof. Recall that $S = \sum_{j2[\eta^\ell]} s_j$. Let neuron $j\ 2\ [\eta^\ell]$ be selected on iteration k of Line 19. For any $k\ 2\ [m]$ we have:

$$\begin{aligned}
Y_k(\mathbf{x}) &= \frac{w_{ij} a_j(\mathbf{x})}{m p_j} \\
&= S\, \frac{w_{ij} a_j(\mathbf{x})}{m\, s_j} \\
&\quad C\, S\, \frac{w_{ij} a_j(\mathbf{x})}{m\, \max_{i^0} g_{i^0 j}(\mathbf{x})} \\
&\quad C\, S\, \frac{w_{ij} a_j(\mathbf{x})}{m\, g_{ij}(\mathbf{x})} \\
&= \frac{C\, S\, z}{m},
\end{aligned}$$

where the first inequality follows by the inequality of event G, the second by the fact that $\max_{i^0} g_{i^0 j}(\mathbf{x}) \quad g_{ij}(\mathbf{x})$ for any i, and the third equality by definition of $g_{ij}(\mathbf{x}) = w_{ij} a_j(\mathbf{x})/z(\mathbf{x})$. This implies that $jY_k \quad \mathsf{E}[Y_k]j = \left|Y_k \quad \frac{z}{m}\right| 2\ [\ z/m, CSz/m]$ by Lemma 3 and since $Y_k \quad 0$. The result follows since $C, S \quad 1$. □

Lemma 6. *For any* $\mathbf{x}$ *such that event* G *occurs, then* $\mathsf{Var}(Y_k(\mathbf{x})) \quad CSz^2/m^2$. *Here the expectation is over the randomness of Algorithm 2.*

Proof. We can use the same inequality obtained by conditioning on G to bound the variance of our estimator.

$$\begin{aligned}
\mathsf{Var}(Y_k(\mathbf{x})) &= \mathsf{E}[Y_k^2(\mathbf{x})] \quad (\mathsf{E}[Y_k(\mathbf{x})])^2 \\
&\quad \mathsf{E}[Y_k^2(\mathbf{x})] \\
&= \sum_{j2[\eta^\ell]} \left(\frac{w_{ij} a_j(\mathbf{x})}{m\, p_j}\right)^2 p_j && \text{by definition of } Y_k \\
&= \frac{S}{m^2} \sum_{j2[\eta^\ell]} \frac{(w_{ij} a_j(\mathbf{x}))^2}{s_j} && \text{since } p_j = s_j/S \\
&\quad \frac{CS}{m^2} \sum_{j2[\eta^\ell]} \frac{(w_{ij} a_j(\mathbf{x}))^2}{\max_{i^0 2[\eta^{\ell+1}]} g_{i^0 j}(\mathbf{x})} && \text{by occurrence of event } \mathsf{G} \\
&\quad \frac{CS\, z}{m^2} \sum_{j2[\eta^\ell]} w_{ij} a_j(\mathbf{x}) && \text{since } g_{ij}(\mathbf{x}) = w_{ij} a_j(\mathbf{x})/z(\mathbf{x}) \\
&= \frac{CSz^2}{m^2}.
\end{aligned}$$

□

We are now ready to prove Theorem 2.

Proof of Theorem 2. Recall the form of Bernstein's inequality that, given random variables $X_1, \ldots, X_m$ such that for each $k \in [m]$ we have $\mathbb{E}[X_k] = 0$ and $|X_k| \leq M$ almost surely, then

$$\mathbb{P}\left(\sum_{k \in [m]} X_k \geq t\right) \leq \exp\left(\frac{t^2/2}{\sum_{k \in [m]} \mathbb{E}[X_k^2] + Mt/3}\right)$$

We apply this with $X_k = Y_k - \frac{z}{m}$. We must take the probability with respect to the randomness of both drawing $\mathbf{x} \sim D$ and Algorithm 2. By Lemma 3, $E[X_k] = 0$. Let us assume that event $\mathcal{G}$ occurs. By Lemma 5, we may set $M = CSz/m$. By Lemma 6, $\sum_{k \in [m]} \mathbb{E}[X_k^2] \leq CSz^2/m$. We will apply the inequality with $t = \varepsilon z$.

Observe that $\sum_{k \in [m]} X_k = \hat{z} - z$. Plugging in these values, and taking both tails of the inequality, we obtain:

$$\begin{aligned}
\mathbb{P}(|\hat{z} - z| \geq \varepsilon z \mid \mathcal{G}) &\leq 2\exp\left(\frac{\varepsilon^2 z^2/2}{CSz^2/m + CS\varepsilon z^2/3m}\right) \\
&= 2\exp\left(\frac{\varepsilon^2 m}{SK(6 + 2\varepsilon)}\right) && \text{since } C \geq 3K \\
&\leq \frac{\delta}{2\eta^{\ell+1}} && \text{by definition of } m
\end{aligned}$$

Removing dependence on event $\mathcal{G}$, we write:

$$\begin{aligned}
\mathbb{P}(|\hat{z} - z| \geq \varepsilon z) &\leq \mathbb{P}(|\hat{z} - z| \geq \varepsilon z \mid \mathcal{G}) + \mathbb{P}(\mathcal{G}) \leq \left(1 - \frac{\delta}{2\eta^{\ell+1}}\right) + \left(1 - \frac{\delta}{2\eta^{\ell+1}}\right) \\
&\leq 1 - \frac{\delta}{\eta^{\ell+1}}
\end{aligned}$$

where we have applied Lemma 4. This implies the result for any single neuron, and the theorem follows by application of the union bound over all $\eta^{\ell+1}$ neurons in layer ℓ. □

B.1 Boosting Sampling via Deterministic Choices

Importance sampling schemes, such as the one described above, are powerful tools with numerous applications in Big Data settings, ranging from sparsifying matrices Baykal et al. (2018); Achlioptas et al. (2013); Drineas & Zouzias (2011); Kundu & Drineas (2014); Tropp et al. (2015) to constructing coresets for machine learning problems Braverman et al. (2016); Feldman & Langberg (2011); Bachem et al. (2017). However, by the nature of the exponential decay in probability associated with importance sampling schemes (see Theorem 1), sampling schemes perform truly well when the sampling pool and the number of samples is sufficiently large Tropp et al. (2015). However, under certain conditions on the sampling distribution, the size of the sampling pool, and the size of the desired sample m, it has been observed that deterministically picking the m samples corresponding to the highest m probabilities may yield an estimator that incurs lower error McCurdy (2018); Papailiopoulos et al. (2014).

To this end, consider a hybrid scheme that picks k indices deterministically (without reweighing) and samples m' indices. More formally, let $C_{\text{det}} \subset [n]$ be the set of k unique indices (corresponding to weights) that are picked deterministically, and define

$$\hat{z}_{\text{det}} = \sum_{j \in C_{\text{det}}} w_{ij} a_j,$$

where we note that the weights are not reweighed. Now let C_{rand} be a set of m' indices sampled from the remaining indices i.e., sampled from $[n] \setminus C_{\text{det}}$, with probability distribution $q = (q_1, \ldots, q_n)$.

To define the distribution q, recall that the original distribution p is defined to be $p_i = s_i/S$ for each $i \in [n]$. Now, q is simply the normalized distribution resulting from setting the probabilities associated with indices in C_{det} to be 0, i.e.,

$$q_i = \begin{cases} \frac{s_i}{S - S_k} & \text{if } i \notin C_{\text{det}}, \\ 0 & \text{otherwise} \end{cases},$$

where $S_k = \sum_{j \in C_{\text{det}}} s_j$ is the sum of sensitivities of the entries that were deterministically picked.

Instead of doing a combinatorial search over all $\binom{n}{k}$ choices for the deterministic set C_{det}, for computational efficiency, we found that setting C_{det} to be the indices with the top k sensitivities was the most likely set to satisfy the condition above.

We state the general theorem below.

Theorem 7. *It is better to keep k feature maps, $C_{\text{det}} \subseteq [\eta^\ell]$, $|C_{\text{det}}| = k$, deterministically and sample $m' = \lceil (6 + 2\varepsilon)(S^\ell - S_k^\ell) K \log(8\eta^\ell/\delta)\varepsilon^{-2} \rceil$ features from $[\eta^\ell] \setminus C_{\text{det}}$ if*

$$\sum_{j \notin C_{\text{det}}} \left(1 - \frac{s_j}{S - S_k}\right)^{m'} > \sum_{j=1}^{\eta^\ell} \left(1 - \frac{s_j}{S}\right)^{m} + \sqrt{\frac{\log(2/\delta)(m + m')}{2}},$$

where $m = \lceil (6 + 2\varepsilon) S^\ell K \log(4\eta^\ell/\delta)\varepsilon^{-2} \rceil$, $S_k = \sum_{j \in C_{\text{det}}} s_j$ and $\eta^\ell = \max_\ell \eta^\ell$.

Proof. Let $m \geq \lceil (6 + 2\varepsilon) S^\ell K \log(4\eta^\ell/\delta)\varepsilon^{-2} \rceil$ as in Lemma 2 and note that from Lemma 2, we know that if $\hat{z}$ is our approximation with respect to sampled set of indices, C, we have

$$\mathbb{P}(E) \geq 1 - \delta$$

where E is the event that the inequality

$$\left|\hat{z}_i^{\ell+1}(x) - z_i^{\ell+1}(x)\right| \leq \varepsilon z_i^{\ell+1}(x) \quad \forall i \in [\eta^{\ell+1}]$$

holds. Henceforth, we will let $i \in [\eta^{\ell+1}]$ be an arbitrary neuron and, similar to before, consider the problem of approximating the neuron's value $z_i^{\ell+1}(x)$ (subsequently denoted by z) by our approximating $\hat{z}_i^{\ell+1}(x)$ (subsequently denoted by $\hat{z}$).

Similar to our previous analysis of our importance sampling scheme, we let $C_{\text{rand}} = \{c_1, \ldots, c_{m'}\}$ denote the multiset of m' neuron indices that are sampled with respect to distribution q and for each $j \in [m']$ define $Y_j = w_{ic_j} a_{c_j}$ and let $Y = \sum_{j \in [m']} Y_j$. For clarity of exposition, we define $\hat{z}_{\text{rand}} = Y$ be our approximation with respect to the random sampling procedure, i.e.,

$$\hat{z}_{\text{rand}} = \sum_{j \in C_{\text{rand}}} w_{ij} a_j = Y.$$

Thus, our estimator under this scheme is given by

$$\hat{z}' = \hat{z}_{\text{det}} + \hat{z}_{\text{rand}}$$

Now we want to analyze the sampling complexity of our new estimator $\hat{z}'$ so that

$$\mathbb{P}(|\hat{z}' - z| \geq \varepsilon z) \leq \delta/2.$$

Establishing the sampling complexity for sampling with respect to distribution q is almost identical to the proof of Theorem 2. First, note that $\mathbb{E}[\hat{z}' \mid \mathbf{x}] = \hat{z}_{\text{det}} + \mathbb{E}[\hat{z}_{\text{rand}} \mid \mathbf{x}]$ since $\hat{z}_{\text{det}}$ is a constant (conditioned on a realization $\mathbf{x}$ of $x \sim D$). Now note that for any $j \in [m']$

$$\begin{aligned} \mathbb{E}[Y_j \mid \mathbf{x}] &= \sum_{k \in [\eta^\ell] \cap C_{\text{det}}} w_{ik} a_k \cdot q_k \\ &= \frac{1}{m'} \sum_{k \in [\eta^\ell] \cap C_{\text{det}}} w_{ik} a_k \end{aligned}$$

$$= \frac{z \quad \hat{z}_{\text{det}}}{m^0},$$

and so $\mathsf{E}[\hat{z}_{\text{rand}} \; j \; \mathbf{x}] = \mathsf{E}[Y \; j \; \mathbf{x}] = z \quad \hat{z}_{\text{det}}$.

This implies that $\mathsf{E}[\hat{z}^0] = \hat{z}_{\text{det}} + (z \quad \hat{z}_{\text{det}}) = z$, and so our estimator remains unbiased. This also yields

$$\begin{aligned} jY \quad \mathsf{E}[Y \; j \; \mathbf{x}]j &= j\hat{z}_{\text{rand}} \quad \mathsf{E}[\hat{z}_{\text{rand}}]j = j\hat{z}_{\text{rand}} + \hat{z}_{\text{det}} \quad zj \\ &= j\hat{z}^0 \quad zj, \end{aligned}$$

which implies that all we have to do to bound the failure probability of the event $jz^0 \quad zj \quad \varepsilon z$ is to apply Bernstein's inequality to our estimator $\hat{z}_{\text{rand}} = Y$, just as we had done in the proof of Theorem 2. The only minor change is the variance and magnitude of the random variables Y_k for $k \; 2 \; [m^0]$ since the distribution is now with respect to q and not p. Proceeding as in the proof of Lemma 5, we have

$$\begin{aligned} \hat{w}_{ij} a_j(\mathbf{x}) = \frac{w_{ij} a_j(\mathbf{x})}{m^0 \, q_j} &= (S \quad S_k) \frac{w_{ij} a_j(\mathbf{x})}{m^0 \, s_j} \\ &\quad \frac{(S \quad S_k) C \, z}{m^0}. \end{aligned}$$

Now, to bound the magnitude of the random variables note that

$$\mathsf{E}[Y_j \; j \; \mathbf{x}] = \frac{z \quad \hat{z}_{\text{det}}}{m^0} = \frac{1}{m^0} \sum_{j \not\in C_{\text{det}}} w_{ij} a_j \quad \frac{(S \quad S_k) C \, z}{m^0}.$$

The result above combined with this fact yields for the magnitude of the random variables

$$R^0 = \max_{j \, 2 \, [m^0]} jY_j \quad \mathsf{E}[Y_j \; j \; \mathbf{x}]j \quad \frac{(S \quad S_k) C \, z}{m^0},$$

where we observe that the only relative difference to the bound of Lemma 5 is the term $S \quad S_k$ appears, where $S_k = \sum_{j 2 C_{\text{det}}} s_j$, instead of S[6]

Similarly, for the variance of a single Y_j

$$\begin{aligned} \mathsf{Var}(Y_j \; j \; \mathbf{x}, G) &\quad \sum_{k 2 [\eta^\ell] n C_{\text{det}}} \frac{(w_{ik} a_k(\mathbf{x}))^2}{m^{02} \, q_k} \\ &= \frac{S \quad S_k}{m^{02}} \sum_{k 2 [\eta^\ell] n C_{\text{det}}} \frac{(w_{ik} a_k(\mathbf{x}))^2}{s_k} \\ &\quad \frac{C(S \quad S_k) \, z}{m^{02}} \sum_{k 2 [\eta^\ell] n C_{\text{det}}} w_{ik} a_k(\mathbf{x}) \\ &\quad \frac{C(S \quad S_k) z^2 \; \min\{1, C(S \quad S_k)\}}{m^{02}}, \end{aligned}$$

where the last inequality follows by the fact that $\sum_{k 2 [\eta^\ell] n C_{\text{det}}} w_{ik} a_k(\mathbf{x}) \quad z$ and by the sensitivity inequality from the proof of Lemma 6

$$\sum_{k 2 [\eta^\ell] n C_{\text{det}}} w_{ik} a_k(\mathbf{x}) \quad Cz \sum_{j 2 [\eta^\ell] n C_{\text{det}}} s_j = Cz(S \quad S_k).$$

This implies by Bernstein's inequality and the argument in proof of Theorem 2 that if we sample

$$m^0 = \lceil (6 + 2\varepsilon) \, (S^\ell \quad S_k^\ell) \, K \, \log(8\eta \; / \delta) \varepsilon^{\; 2} \rceil$$

times from the distribution q, then we have

$$\mathsf{P}(j\hat{z}^0 \quad zj \quad \varepsilon z) \quad \delta/2.$$

[6] and of course the sampling complexity is m^0 instead of m

Now let $p = (p_1, \ldots, p_n)$ be the probability distribution and let C denote the multi-set of indices sampled from $[n]$ when m samples are taken from $[n]$ with respect to distribution p. For each index $j \in [n]$ let $U_j(m,p) = \mathbb{1}[j \in C]$ be the indicator random variable of the event that index j is sampled at least once and let $U(m,p) = \sum_{i=j}^{n} U_j(m,p)$. Note that U is a random variable that denotes the number of unique samples that result from the sampling process described above, and its expectation is given by

$$\begin{aligned}
\mathbb{E}[U(m,p)] &= \sum_{j=1}^{n} \mathbb{E}[U_j(m,p)] = \sum_{j=1}^{n} \mathbb{P}(i \in C) \\
&= \sum_{j=1}^{n} \mathbb{P}(j \text{ is sampled at least once}) \\
&= \sum_{j=1}^{n} (1 - \mathbb{P}(j \text{ is not sampled})) \\
&= n - \sum_{j=1}^{n} (1 - p_j)^m.
\end{aligned}$$

Now we want to establish the condition for which $U(m',q) < U(m,p)$, which, if it holds, would imply that the number of distinct weights that we retain with the deterministic + sampling approach is lower and still achieves the same error and failure probability guarantees, making it the overall better approach. To apply a strong concentration inequality, let $C' = C_{\text{det}} \cup C_{\text{rand}} = \{c'_1, \ldots, c'_k, c'_{k+1}, \ldots, c'_{m'}\}$ denote the set of indices sampled from the deterministic + sampling (with distribution q) approach, and let $C = \{c_1, \ldots, c_m\}$ be the indices of the random samples obtained by sampling from distribution p. Let $f(c'_1, \ldots, c'_{m'}, c_1, \ldots, c_m)$ denote the difference $U(m',q) - U(m,p)$ in the number of unique samples in C' and C. Note that f satisfies the bounded difference inequality with Lipschitz constant 1 since changing the index of any single sample in $C \cup C'$ can change f by at most 1. Moreover, there are $m' + m$ random variables, thus, applying McDiarmid's inequality van Handel (2014), we obtain

$$\mathbb{P}(\mathbb{E}[U(m,p) - U(m',q)] - (U(m,p) - U(m',q)) \geq t) \leq \exp\left(\frac{-2t^2}{(m+m')}\right),$$

this implies that for $t = \sqrt{\frac{\log(2/\delta)(m+m')}{2}}$,

$$\mathbb{E}[U(m,p) - U(m',q)] - U(m,p) - U(m',q) + t$$

with probability at least $1 - \delta/2$. Thus, this means that if $E[U(m,p)] - \mathbb{E}[U(m',q)] > t$, then $U(m,p) > U(m',q)$.

More specifically, recall that

$$\mathbb{E}[U(m,p)] = n - \sum_{j=1}^{n} (1 - p_j)^m = n - \sum_{j=1}^{n} \left(1 - \frac{s_j}{S}\right)^m$$

and

$$\begin{aligned}
\mathbb{E}[U(m',q)] &= k + \sum_{j:q_j>0} (1 - (1 - q_j)^{m'}) \\
&= k + (n - k) - \sum_{j:q_j>0} (1 - q_j)^{m'} \\
&= n - \sum_{j:q_j>0} (1 - q_j)^{m'} \\
&= n - \sum_{j \notin C_{\text{det}}} \left(1 - \frac{s_j}{S - S_k}\right)^{m'}
\end{aligned}$$

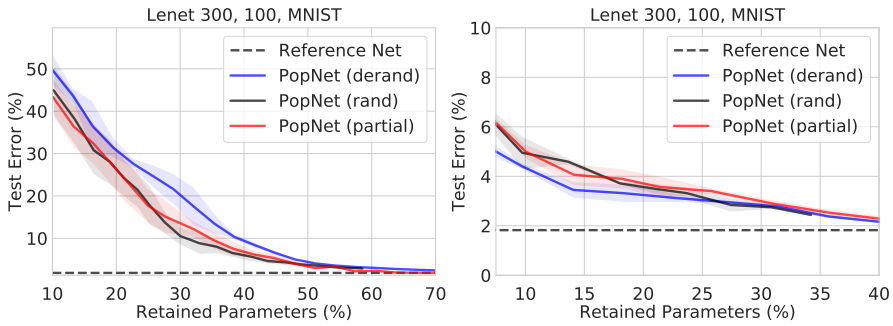

(a) Before retraining (b) After retraining

Figure 5: The performance of our approach (PopNet) on a LeNet300-100 architecture trained on MNIST with no derandomization (denoted by "rand"), with partial derandomization (denoted by "partial"), and with complete derandomization (denoted by "derand"). The plot in (a) and (b) show the resulting test accuracy for various percentage of retained parameters 1 (pruneratio) before and after retraining, respectively. The additional error of the derandomized algorithm can be neglected in practical settings, especially after retraining.

Thus, rearranging terms, we conclude that it is better to conduct the deterministic + sampling scheme if

$$\sum_{j \notin C_{\text{det}}} \left(1 - \frac{s_j}{S - S_k}\right)^{m^0} > \sum_{j=1}^{n} \left(1 - \frac{s_j}{S}\right)^{m} + \sqrt{\frac{\log(2/\delta)(m + m^0)}{2}}.$$

Putting it all together, and conditioning on the above inequality holding, we have by the union bound

$$\mathsf{P}(j \hat{z}^0 \quad zj \quad \varepsilon z \; [\; U(m^0, q) > U(m, p)) \quad \delta,$$

this implies that with probability at least 1 δ: (i) $\hat{z}^0$ 2 (1 ε)z and (ii) $U(m^0, q) < U(m, p)$, implying that the deterministic + sampling approach ensures the error guarantee holds with a smaller number of unique samples, leading to better compression. □

B.1.1 Experimental Evaluation of Derandomization

To evaluate our theoretical results of derandomization, we tested the performance of our algorithm with respect to three different variations of sampling:

1. No derandomization ("rand"): We apply Alg. 2 and sample channels with probability proportional to their sensitivity.
2. Partial derandomization ("partial"): We apply Theorem 7 as a preprocessing step to keep the top k channels and then sample from the rest according to Alg. 2.
3. Complete derandomization ("derand"): We simply keep the top channels until our sampling budget is exhausted.

The results of our evaluations on a LeNet300-100 architecture trained on MNIST can be seen in Fig. 5. As visible from Fig. 5(a), the process of partial derandomization does not impact the performance of our algorithm, while the complete derandomization of our algorithm has a slightly detrimental effect on the performance. This is in accordance to Theorem 7, which predicts that that it is best to only partially derandomize the sampling procedure. However, after we retrain the network, the additional error incurred by the complete derandomization is negligible as shown in Fig. 5(b). Moreover, it appears that – especially for extremely low sampling regime – the completely derandomized approach seems to incur a slight performance boost relative to the other approaches. We suspect that simply keeping the top channels may have a positive side effect on the optimization landscape during retraining, which we would like to further investigate in future research.

C MAIN COMPRESSION THEOREM

Having established layer-wise approximation guarantees as in Sec. B, all that remains to establish guarantees on the output of the entire network is to carefully propagate the error through the layers as was done in Baykal et al. (2018). For each $i \in [\eta^{\ell+1}]$ and $\ell \in [L]$, define

$$\tilde{} {}^{\ell}_{i}(x) = \left(z_i^{+}(x) + z_i(x)\right)/_{|z_i(x)|},$$

where $z_i^{+}(x) = \sum_{k \in I^{+}} w_{ik}^{\ell+1} a_k^{\ell}(\mathbf{x})$ and $z_i(x) = \sum_{k \in I^{-}} w_{ik}^{\ell+1} a_k^{\ell}(\mathbf{x})$ are positive and negative components of $z_i^{\ell+1}(x)$, respectively, with I^{+} and I^{-} as in Alg. 2. For each $\ell \in [L]$, let $\quad^{\ell}$ be a constant defined as a function of the input distribution D [7], such that with high probability over $x \sim D$, $\quad^{\ell} \geq \max_{i \in [\eta^{\ell+1}]} \quad^{\ell}_{i}$. Finally, let $\quad^{\ell\,!} = \prod_{k=\ell}^{L} \quad^{k}$.

We now apply the error propagation bounds of Baykal et al. (2018) to conclude our main compression theorem below.

Theorem 8. *Let $\varepsilon, \delta \in (0,1)$ be arbitrary, let $S \geq X$ denote the set of $d K^{0} \log(4\eta/\delta) e$ i.i.d. points drawn from D, and suppose we are given a network with parameters $\theta = (W^1, \ldots, W^L)$. Consider the set of parameters $\hat{\theta} = (\hat{W}^1, \ldots, \hat{W}^L)$ generated by pruning channels of θ according to Alg. 2 for each $\ell \in [L]$. Then, $\hat{\theta}$ satisfies*

$$\mathop{\mathsf{P}}_{\hat{\theta}, x \sim D}\left(f_{\hat{\theta}}(x) \in (1 \pm \varepsilon) f_{\theta}(x)\right) \geq 1 - \delta,$$

and the number of channels in $\hat{\theta}$ is bounded by

$$O\left(\sum_{\ell=1}^{L} \frac{L^2 (\quad^{\ell\,!})^2 S^{\ell} \log(\eta/\delta)}{\varepsilon^2}\right).$$

D EXTENSION TO CNNS

To extend our algorithm to CNNs, we need to consider the fact that there is implicit weight sharing involved by definition of the CNN filters. Intuitively speaking, to measure the importance of a feature map (i.e. neuron) in the case of FNNs we consider the maximum impact it has on the preactivation $z^{\ell+1}(x)$. In the case of CNNs the same intuition holds, that is we want to capture the maximum contribution of a feature map $a_j^{\ell}(x)$, which is now a two-dimensional image instead of a scalar neuron, to the pre-activation $z^{\ell+1}(x)$ in layer $\ell + 1$. Thus, to adapt our algorithm to prune channels in CNNs, we modify the definition of sensitivity slightly, by also taking the maximum over the patches $p \in P$ (i.e., sliding windows created by convolutions). In this context, each activation $a_j^{\ell}(x)$ is also associated with a patch $p \in P$, which we denote by a_{jp}^{ℓ}. In particular, the slight change is the following:

$$s_j^{\ell} = \max_{x \in S} \max_{i \in [\eta^{\ell+1}]} \max_{p \in P} \frac{w_{ij}^{\ell+1} a_{jp}^{\ell}(x)}{\sum_{k \in [\eta^{\ell}]} w_{ik}^{\ell+1} a_{kp}^{\ell}(x)},$$

where $a_{\ p}$ corresponds to the activation window associated with patch $p \in P$. Everything else remains the same and the proofs are analogous.

E ADDITIONAL EXPERIMENTAL DETAILS

For our experimental evaluations, we considered a variety of data sets (MNIST, CIFAR10) and neural network architectures (LeNet, VGG, ResNet, WideResNet, DenseNet) and compared against several state-of-the-art filter pruning methods. We conducted all experiments on a single NVIDIA GTX 1080Ti with 11GB RAM and implemented them in PyTorch Paszke et al. (2017).

In the following, we summarize our hyperparameters for training and give an overview of the comparison methods. All reported experimental quantities are averaged over three separately trained and pruned networks.

[7] If $\quad_i(x)$ is a sub-Exponential random variable Vershynin (2016) with parameter $\lambda = O(1)$, then for δ failure probability: $\quad^{\ell} = O(\mathsf{E}_{x \sim D}[\max_i \quad_i(x)] + \log(1/\delta))$ Baykal et al. (2018); Vershynin (2016)

E.1 COMPARISON METHODS

We further evaluated the performance of our algorithm against a variety of state-of-the-art methods in filter pruning as listed below. We note that for all presented results for network configurations appearing in the respective related work we compare against their reported pruning performance. For experiments not considered, we report the performance from our own experiments. Note that for our own experiments, we deployed the same simple one-shot pruning and fine-tune strategy as is used in our method to ensure an objective comparison method. Moreover, we considered a fixed pruning ratio of filters in each layers as none of the competing methods provide an automatic procedure to detect relative layer importance and allocate samples accordingly. Thus, the differentiating factor between the competing methods is their respective pruning step that we elaborate upon below.

Filter Thresholding (FT, Li et al. (2016) Consider the set of filters $W^\ell = [W_1^\ell, \ldots, W_{\eta^\ell}^\ell]$ in layer ℓ and let $\left\|W_j^\ell\right\|_{2,2}$ denote the entry-wise ℓ_2-norm of W_j^ℓ (or Frobenius norm). Consider a desired sparsity level of t%, i.e., we want to keep only t% of the filters. We then simply keep the filters with the largest norm until we satisfy our desired level of sparsity.

SoftNet (He et al., 2018) The pruning procedure of. He et al. (2018) is similar in nature to Li et al. (2016) except the saliency score used is the entrywise ℓ_1 - norm $\left\|W_j^\ell\right\|_{1,1}$ of a filter map W_j^ℓ. During their fine-tuning scheme they allow pruned filters to become non-zero again and then repeat the pruning procedure. As for the other comparisons, however, we only employ one-shot prune and fine-tune scheme.

ThiNet (Luo et al., 2017) Unlike the previous two approaches, which compute the saliency score of the filter W_j^ℓ by looking at its entry-wise norm, the method of Luo et al. (2017) iteratively and greedily chooses the feature map (and thus corresponding filter) that incurs the least error in an absolute sense in the pre-activation of the next layer. That is, initially, the method picks filter j such that $j = \mathsf{argmin}_{j2[\eta^\ell]} \mathsf{max}_{x2S} \left| z^{\ell+1}(x) \quad z_{[j]}^{\ell+1}(x) \right|$, where $z^{\ell+1}(x)$ denotes the pre-activation of layer $\ell + 1$ for some input data point x, $z_{[j]}^{\ell+1}(x)$ the pre-activation when only considering feature map j in layer ℓ, and S a set of input data points. We note that this greedy approach is quadratic in both the size η^ℓ of layer ℓ and the size jSj of the set of data points S, thus rendering it very slow in practice. In particular, we only use a set S of cardinality comparable to our own method, i.e., around 100 data points in total. On the other hand, Luo et al. report to use 100 data points per output class resulting in 1000 data points for CIFAR10.

Learning to prune (LearnNet, Huang et al. (2018)) LearnNet leverages a form of reinforcement learning to learn the optimal substructure in each layer, i.e., it aims to learn which filters are optimally pruned. We did not implement this comparison methods due to large computational cost of the method (around 480 GPU hours for one experiment on CIFAR10) but rather only mention results from experiments that were directly reported in Huang et al. (2018).

E.2 LENET ARCHITECTURES ON MNIST

We evaluated the performance of our pruning algorithm, denoted *PopNet*, and the comparison methods on LeNet300-100 (LeCun et al., 1998), a fully-connected network with two hidden layers of size 300 and 100 hidden units, respectively, and its convolutional counterpart, LeNet-5 (LeCun et al., 1998), which consists of two convolutional layers and two fully-connected layers. Both networks were trained on MNIST using the hyper-parameters specified in Table 3. We trained on a single GPU and during retraining (fine-tunine) we maintained the same hyperparameters and only adapted the ones specifically mentioned in Table 3.

E.3 CONVOLUTIONAL NEURAL NETWORKS ON CIFAR-10

We further evaluated the performance of our algorithm on a variety of convolutional neural network architectures trained on CIFAR10. Specifically, we tested it on VGG16 (Simonyan & Zisserman, 2014b), ResNet20 (He et al., 2016), DenseNet22 (Huang et al., 2017), and Wide ResNet-16-8 (Zagoruyko &

		LeNet-300-100	LeNet-5
Train	test error	1.59	0.70
	loss	cross-entropy	cross-entropy
	optimizer	SGD	SGD
	epochs	40	40
	batch size	64	64
	LR	0.01	0.01
	LR decay	0.1@{30}	0.1@{25, 35}
	momentum	0.9	0.9
	weight decay	1.0e-4	1.0e-4
Fine-tune	epochs	30	30
	LR decay	0.1@{20, 28}	0.1@{20, 28}

Table 3: We report the hyperparameters used during MNIST training for the LeNet architectures. LR hereby denotes the learning rate and LR decay denotes the learning rate decay that we deploy after a certain number of epochs. During fine-tuning (FT) we used the same hyperparameters except for the ones indicated in the lower part of the table.

Komodakis, 2016). For residual networks with skip connections, we model the interdependencies between the feature maps and only prune a feature map if it does not get used as an input in the subsequent layers. We performed the training on a single GPU using the same hyperparameters specified in the respective papers for CIFAR training with the exception of the batch size in case we need to account for the limited memory in a single GPU. During fine-tuning we reduced the number of epochs and also adjusted the learning rate schedule accordingly while keeping all other parameters unchanged. We summarize the set of hyperparameters for the various networks in Table 4.

		VGG16	ResNet20	DenseNet22	WRN-16-8
Train	test error	8.46	8.76	13.75	9.37
	loss	cross-entropy	cross-entropy	cross-entropy	cross-entropy
	optimizer	SGD	SGD	SGD	SGD
	epochs	300	182	120	120
	batch size	256	128	64	64
	LR	0.05	0.1	0.1	0.1
	LR decay	0.5@{30, . . . }	0.1@{91, 136}	0.1@{60, 90}	0.2@{30, . . . }
	momentum	0.9	0.9	0.9	0.9
	Nesterov			✓	✓
	weight decay	5.0e-4	1.0e-4	1.0e-4	5.0e-4
Fine-tune	epochs	150	182	40	120
	LR decay	0.5@{30, . . . }	0.1@{91, 136}	0.1@{20, 30}	0.2@{15,22, 27}

Table 4: We report the hyperparameters used during training for various convolutional architectures on CIFAR10. LR hereby denotes the learning rate and LR decay denotes the learning rate decay that we deploy after a certain number of epochs. During fine-tuning we used the same hyperparameters except for the ones indicated in the lower part of the table. $f30, \ldots g$ denotes that the learning rate is decayed every 30 epochs.

E.4 Application to Real-time Regression Tasks

In the context of autonomous driving and other real-time applications of neural network inference, fast inference times while maintaining high levels of accuracy are paramount to the successful deployment of such systems (Amini et al., 2018). The particular challenge of real-time applications stems from the fact that – in addition to the conventional trade-off between accuracy and model efficiency – inference has to be conducted in real-time. In other words, there is a hard upper bound on the allotted computation time before an answer needs to be generated by the model. Model compression, and in particular, filter compression can provide a principled approach to generating high accuracy

	test loss	loss	optimizer	epochs	batch size	LR	LR decay	weight decay
Deepknight	0.49	MSE	Adam	100	32	1e-4	0.1@{50, 90}	1e-4

Table 5: We report the hyperparameters used during the driving network of Amini et al. (2018) together with the provided data set. No retraining was conducted for this architecture MNIST training for the LeNet architectures. LR hereby denotes the learning rate, LR decay denotes the learning rate decay that we deploy after a certain number of epochs, and MSE denotes the mean-squared error.

outputs without incurring high computational cost. Moreover, the provable nature of our approach is particularly favorable for real-time applications, as they usually require extensive performance guarantees before being deployed, e.g., autonomous driving tasks.

To evaluate the empirical performance of our filter pruning method on real-time systems, we implemented and tested the neural network of Amini et al. (2018), which is a regression neural network deployed on an autonomous vehicle in real time to predict the steering angle of the human driver. We trained the network of Amini et al. (2018), denoted by *Deepknight*, with the driving data set provided alongside, using the hyperparameters summarized in Table 5.

The results of our compression can be found in Fig. 6, where we evaluated and compared the performance of our algorithm to those of other SOTA methods (see Sec. E.1). We note that these results were achieved *without* retraining as our experimental evaluations have shown that even without retraining we can achieve significant pruning ratios that lead to computational speed-ups in practice. As apparent from Fig. 6, we can again outperform other SOTA methods in terms of performance vs. prune ratio. Note that since this is a regression task, we used test loss (mean-squared error on the test data set) as performance criterion.

Finally, we would like to highlight that our filter pruning method may serve as a principled subprocedure during the design of neural network architectures for real-time applications. In particular, given an inference time budget T, one can design and train much larger architectures with favorable performance which, however, violate the given budget T. Our filter pruning method can then be leveraged to compress the network until the given budget T is satisfied, thus reducing the burden on the practitioner to design a simultaneously accurate and computationally-efficient neural network architecture.

(a) Example driving image from Amini et al. (2018)

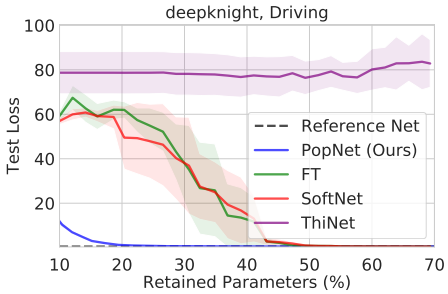

(b) Pruning performance before retraining

Figure 6: The performance of our approach (PopNet) on a regression task used to infer the steering angle for an autonomous driving task (Amini et al., 2018). (a) An exemplary image taken from the data set. (b) The performance of our pruning procedure before retraining evaluated on the test loss and compared to competing filter pruning methods. Note that the x axis is percentage of parameters retained, i.e., 1 (pruneratio).